ORIGINAL PAPER

Available from: http://www.jgld.ro/wp/archive/y2017/n4/a13/
DOI: http://dx.doi.org/10.15403/jgld.2014.1121.264.nin

Nodule-in-Nodule Imaging Pattern in Hepatocellular Carcinoma Treated by Transarterial Chemoembolization – a Multiparametric Magnetic Resonance Imaging Study

Andreea E. Scheau[1], Cristian Scheau[2], Ioana G. Lupescu[1,2]

1) Department of Radiology, Medical Imaging and Interventional Radiology, Fundeni Clinical Institute, Bucharest
2) Carol Davila University of Medicine and Pharmacy, Bucharest, Romania

Address for correspondence:
Andreea-Elena Scheau, MD
Department of Radiology, Medical Imaging and Interventional Radiology, Fundeni Clinical Institute, 258 Fundeni Street
Bucharest, Romania
andreea.ghergus@gmail.com

Received: 10.07.2017
Accepted: 25.10.2017

ABSTRACT

Background & Aims: Emerging minimally invasive treatments for hepatocellular carcinoma (HCC) can significantly improve a patient's prognosis, but they may alter the imaging features of the treated nodules. This study focuses on a series of patients presenting with a rare pathology, the nodule-in-nodule imaging pattern of HCC, analyzes the imaging features and discusses possible approaches for the diagnosis of tumoral recurrence.
Method: Nine patients recruited over two years, having HCC with nodule-in-nodule imaging pattern on diagnosis, and treated by transarterial chemoembolization were monitored by magnetic resonance imaging (MRI). Nodule morphology, dynamic contrast behavior and size progression were followed in this study.
Results: All patients showed tumor recurrence. In 7 nodules, a T2 weighted-imaging hyperintense signal of the HCC foci was found, with isointensity of the background nodule. Restricted diffusion within the HCC foci was found in 6 cases but with no statistical significance. Dynamic contrast images evaluation showed a "classical" enhancement pattern in five patients. All nodules had hypointense HCC foci in the hepatobiliary phase. Four patients demonstrated progressive disease according to the mRECIST criteria.
Conclusions: Due to the particularly challenging nodule characteristics, the sensitivity in diagnosing HCC foci in these nodules is about 77% when using conventional imaging criteria related to nodule morphology. Contrast media uptake curves may be altered by changes in nodule hemodynamics caused by embolization. The diagnostic rate may be significantly increased by considering the tumoral size increase in follow-up studies and completing the study with a hepatobiliary phase using Acidum Gadoxeticum.

Key words: Nodule-in-nodule – transarterial chemoembolization – hepatocellular carcinoma – magnetic resonance imaging – image analysis –Acidum Gadoxeticum.

Abbreviations. ADC: Apparent diffusion coefficient; CT: Computed tomography; DEB-TACE: drug-eluting beads transarterial chemoembolization; DWI: Diffusion-weighted imaging; Gd-EOB-DTPA: acidum gadoxeticum; HCC: hepatocellular carcinoma; HBV: hepatitis virus B; HCV: hepatitis virus C; HDV: hepatitis virus D; IN-OPP: in-phase and out-of-phase; mRECIST: modified Response Evaluation Criteria in Solid Tumors; MRI: Magnetic resonance imaging; ROI: region of interest; TACE: Transarterial chemoembolization; WI: weighted imaging.

INTRODUCTION

Hepatocellular carcinoma (HCC) is the fifth most frequent cancer worldwide, and the leading cause of death in patients with liver cirrhosis [1]. The most recent practice guidelines state that histological evidence is no longer necessary to confirm a HCC if the tumor is larger than 10 mm and shows typical imaging features on contrast enhanced computed tomography (CT) or magnetic resonance imaging (MRI)[2].

Transarterial chemoembolization (TACE) is the preferred method for treating intermediate stage HCC [3, 4], being widely used [5]. There is continued interest for its various procedures and chemotherapeutic agents used despite potential risks and complications [6]. After the successful occlusion of the arterial blood flow of the malignant nodule, the portal blood regurgitation into the adjacent sinusoid vessels may favor tumor remnants, thus reducing the efficacy of TACE [7, 8].

A relatively rare imaging pattern found in patients with TACE for HCC developed on a cirrhotic liver is the "nodule-in-nodule" appearance, which has an incidence of about 6%

in untreated patients [9]. This refers to HCC foci in a highly dysplastic nodule, and holds particular importance, since for a correct depiction one must surpass several diagnostic pitfalls. Furthermore, the availability of morphological and functional modalities for MRI, as well as hepatocyte-specific contrast media, allows a highly accurate diagnosis based on clear imaging criteria [10].

The goals of this paper are to describe the MRI profiles of patients treated with TACE for an HCC with "nodule-in-nodule" imaging features, and to identify the potential obstacles in the correct diagnosis of tumor recurrence.

PATIENTS AND METHODS

Nine patients (M/F: 4/5, aged 55 to 74 years old, mean age 64 years) with HCC on a cirrhotic liver treated with TACE recruited between January 2014 and December 2016 are evaluated in this study. Their baseline imaging scan, CT or MRI showed a "nodule-in-nodule" pattern. These patients underwent contrast enhanced MRI at four weeks after the embolization, as part of their follow-up management protocol. None of the patients were candidates for other minimally invasive procedures such as radiofrequency ablation or microwave ablation due to the presence of multinodular or intermediate stage HCC, which directs the treatment towards TACE, exclusively [11].

The follow-up MRI at four weeks used a Toshiba Vantage Titan 1,5 Tesla MRI platform with a dedicated Workstation. The protocol is shown in Table I. Dynamic contrast media administration was performed using Acidum Gadoxeticum 0.1ml/kg in five steps: unenhanced phase, arterial phase (30 seconds delay after the start of contrast media iv. injection), portal venous phase (70 seconds delay), late (transitional) phase (180 seconds delay) and hepatobiliary phase (20 minutes delay), followed by a 20 ml serum bolus, both with a perfusion rate of 1 ml/second.

The images for all the 9 patients were evaluated using the dedicated certified imaging software OsiriX 8.0.2 MD 64bit. The measurement of the signal intensity in the background nodule and in the HCC foci was performed using an elliptical region of interest (ROI) in the most homogeneous zone, with the largest possible area between 0.1 and 1 cm^2 according to the lesion size.

Arterial flash was defined as a vivid early arterial enhancement of the lesion compared to the remainder of the liver, while contrast wash-out as an early hypointensity of the lesion compared to the rest of the liver parenchyma [12]. Diffusion restriction is defined as an objective hyperintensity of the lesion in all b-values, including the highest, with corresponding hypointensity on the ADC map [13].

The nodule volume was estimated using the following formula for determining an ellipsoid volume based on three diameters: V = length * width * height * π/6.

Statistical data was analyzed using IBM SPSS Statistics 21 Premium x64bit. The data was tested for normality using Shapiro-Wilk Normality Test, and all data groups seemed normal for thresholds of p between 0.01 and 0.10 with accepted null hypothesis [14]. Chi-square test and Fisher's exact test were used for testing contingency tables, the latter being used when the minimum value in a cell was zero. Mann-Whitney's test for independent samples was used to determine if sets of data between sub-lots demonstrate significant differences. Due to the small sample size, Spearman's correlation coefficient was chosen in favor of Pearson's to test correlations between continuous variables.

All the patients enrolled in this study signed a written informed consent, and the study was approved by the local Ethics Committee.

RESULTS

The 9 patients included in the study presented background nodules with an average size of 41.1 ± 11.1 mm in the largest diameter, and an estimated volume of 27.4 ± 19.14 cc. The HCC foci measured in average 14.7 ± 3.16 mm and had a mean volume of 1.29 ± 0.95 cc.

Size comparison in the HCC foci between the baseline examination and the post-procedural MRI investigation was performed. The results were expressed in percentages of size increment (Table II). Four patients demonstrated progressive disease according to the mRECIST criteria [15].

Table I. Parameters of the imaging protocol used in this study.

Series no	Sequence name	Imaging plane	TR (ms)	TE (ms)	Slice thickness (mm)	Gap (mm)	Voxel size (mm)
1	T1 IN-OPP PHASE	Transverse	133	2.38/4.76	4.0	0.8	0.8x0.8x4.0
2	T2 HASTE LONG TE	Coronal	3300	383	6.0	1.2	1.2x1.2x6.0
3	T2 HASTE SHORT TE	Coronal	1200	90	4.0	1.2	1.6x1.6x4.0
4	T2 TSE DIXON	Transverse	2000	90	6.0	1.2	1.3x1.3x6.0
5	T2 TSE	Transverse	2500	120	5.0	1.5	1.3x1.3x5.0
6	DWI (b=50,400,800)	Transverse	2000	56	5.0	1.5	1.5x1.5x5.0
7	GRADIENT ECHO (FA=12)	Transverse	250	12	6.0	1.8	0.8x0.8x6.0
8	DYNAMIC T1 FATSAT	Transverse	4.44	2.16	3.0	0.6	1.3x1.3x3.0
9	LATE ENHANCEMENT T1 FATSAT	Transverse	4.44	2.16	3.0	0.6	1.3x1.3x3.0
10	LATE ENHANCEMENT T1 FATSAT	Coronal	6.63	2.39	1.6	0.3	1.6x1.6x1.6
11	T1 FATSAT (FA=30)	Transverse	4.69	2.21	3.0	0.6	1.3x1.3x3.0

TR: time of repetition; TE: time of echo; IN-OPP: in-phase and out-of-phase; TSE: turbo spin echo; FA: flip angle; FATSAT: fat saturation.

Analyzing the nodule morphology in T2 WI, 7 out of the 9 nodules demonstrated a hyperintense signal of the HCC foci with an isointense aspect of the background nodule. Out of these 7, 6 demonstrated restricted diffusion within the HCC foci, with variable ADC values. No nodules showed hypointensity in T2 WI within the HCC foci.

Regarding the T1 WI signal in the HCC foci, 2 nodules showed isointensity in the unenhanced series.

Restricted diffusion within the HCC foci was found in 6 cases, with ADC map values between 901 and 1632 $*10^{-3}$ mm^2/s (averaging 1280 ± 247 $*10^{-3}$ mm^2/s). The tumor nodules without restricted diffusion held ADC values between 1374 and 1783 $*10^{-3}$ mm^2/s (averaging 1579 ± 204 $*10^{-3}$ mm^2/s). There was no statistically significant difference between the two lots when compared with independent sample testing (p=0.1667). However, the presence of diffusion restriction marginally correlated positively with T2 hyperintensity in the HCC foci (p = 0.083).

Dynamic contrast images evaluation showed a "classical" pattern of enhancement in the arterial phase with subsequent wash-out in the late phase in 5 out of 9 patients. The other 4 showed either no contrast wash-out, or continual enhancement in the late phase. All nodules imaged in this study had hypointense HCC foci in the biliary phase.

No statistically significant correlation was found between the tumor nodule size and the degree of contrast enhancement (rho=0.0167, p=0.9661).

The overall patients' characteristics and imaging findings are summarized in Table II.

DISCUSSION

A typical morphological imaging profile of a HCC nodule in the cirrhotic liver consists of hypointensity in T1 WI, hyperintensity in T2 WI, and restricted diffusion with ADC values ranging between 0.7 * 10^{-3} mm^2/s and 1.3 * 10^{-3} mm^2/s [16, 17]. The dynamic contrast profile of this type of tumor nodule demonstrates an intense contrast enhancement in the arterial phase, the so-called "arterial flash" with a decrease of signal intensity in the portal phase (tumoral "wash-out") [18]. HCC nodules are commonly hypointense in the hepatobiliary phase [10, 19]. Using hepatocyte-specific contrast media, especially Acidum Gadoxeticum (Fig. 1), augments these findings and facilitates nodule detection [20].

Table II. Imaging findings of the patients in the study at four weeks after TACE

Patient no.	Age, gender/ Cirrhosis etiology	Nodule-in-nodule area of interest	3-axis sizes (mm)			Volume (cc)	Size increase from baseline (mRECIST criteria)	Morphology				Dynamic contrast		
								T1 WI	T2 WI	Restricted diffusion	ADC value ($*10^{-3}$ mm^2/s)	Contrast wash-in	Contrast wash-out	Hepato-biliary phase
1	60, female	Background nodule	52	31	35	29.53	-	Hyper	Iso	No	-	No	No	Iso
	HVC	HCC foci	11	11	11	0.70	27%	Iso	Iso	No	1783	No	No	Hypo
2	65, female	Background nodule	56	37	64	69.40	-	Hyper	Iso	No	-	No	No	Iso
	HVC	HCC foci	21	16	21	3.69	23%	Hypo	Hyper	No	1580	No	No	Hypo
3	72, female	Background nodule	23	18	18	3.90	-	Hyper	Iso	No	-	No	No	Iso
	HVC	HCC foci	14	9	11	0.73	0%	Hypo	Hyper	Yes	1215	No	No	Hypo
4	58, male	Background nodule	32	26	29	12.63	-	Hyper	Iso	No	-	No	No	Iso
	HVB+D	HCC foci	17	14	13	1.62	8%	Hypo	Iso	No	1374	Yes	Yes	Hypo
5	74, female	Background nodule	44	42	42	40.62	-	Hyper	Iso	No	-	No	No	Hypo
	HVC	HCC foci	13	11	9	0.67	0%	Hypo	Hyper	Yes	1358	Yes	Yes	Hypo
6	65, male	Background nodule	26	20	20	5.44	-	Hyper	Iso	No	-	No	No	Hypo
	HVB+D	HCC foci	11	8	10	0.46	16%	Hypo	Hyper	Yes	901	Yes	Yes	Hypo
7	55, male	Background nodule	42	40	37	32.53	-	Hyper	Iso	No	-	No	No	Hyper
	HVC	HCC foci	16	12	13	1.31	31%	Hypo	Hyper	Yes	1172	Yes	Yes	Hypo
8	66, male	Background nodule	52	36	33	32.33	-	Hyper	Iso	No	-	No	No	Hypo
	HVB+D	HCC foci	17	16	12	1.71	12%	Hypo	Hyper	Yes	1632	No	No	Hypo
9	65, female	Background nodule	43	31	29	20.23	-	Hyper	Iso	No	-	No	No	Iso
	HVC	HCC foci	12	11	10	0.69	20%	Iso	Hyper	Yes	1407	Yes	Yes	Hypo

HBV: hepatitis B virus, HCV: hepatitis C virus, HVD: hepatitis D virus, WI: weighed imaging, ADC: apparent diffusion coefficient, HCC: hepatocellular carcinoma, Hypo: hypointensity, Iso: isointensity, Hyper: hyperintensity.

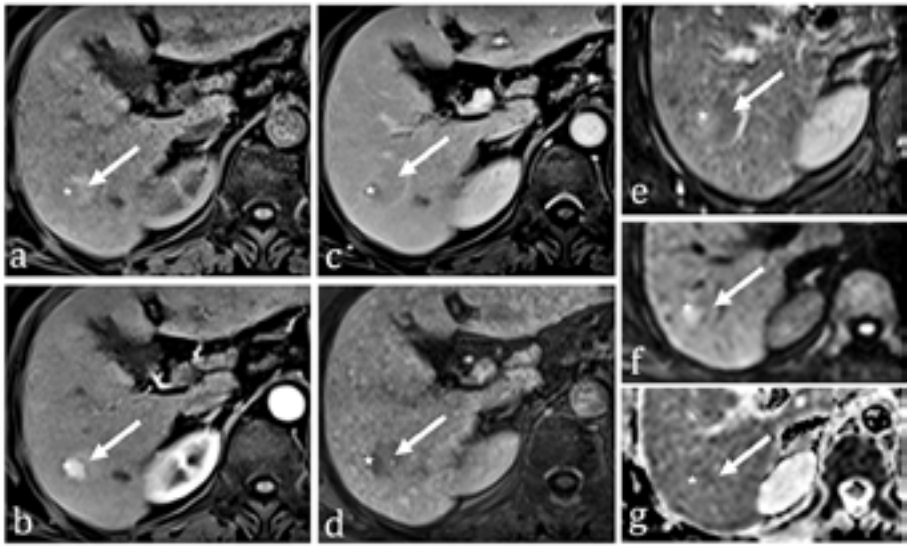

Fig. 1. Images demonstrating a typical tumoral nodule-in-nodule pattern. Dysplastic nodule T1 hyperintense/T2 hypointense, with a tumor nidus in T2 hyperintensity/T1 hypointensity, restricted diffusion, arterial flash and portal venous phase wash-out. Arrow – background nodule, * – HCC foci; T1 FatSat images in unenhanced (a), arterial phase (b), portal venous phase (c), hepatobiliary phase (d); T2 FatSat images (e); DWI images (f) with ADC map correlation (g).

However, these "classical" imaging findings of a HCC nodule may be substantially altered in patients previously submitted to TACE, due to several factors such as the alteration of the blood flow to- and possibly from the nodule, and the appearance of granulation tissue around the nodule [21]. Even more confounding variables may appear when imaging nodule-in-nodule patterns after TACE treated HCC foci (Fig. 2). Few literature data is available regarding the best diagnostic approach in these cases [22].

The nodule-in-nodule architecture is represented by a background nodule, which is usually highly dysplastic but better-differentiated, and a smaller inner-nodule, consisting of small HCC foci with less fat and iron, and poor tumoral cell differentiation [23].

The background nodule appears hyperintense in T1 WI, hypointense in T2 WI, with slight or moderate arterial enhancement, while the inner-nodule shows typical imaging features of a HCC nodule [24].

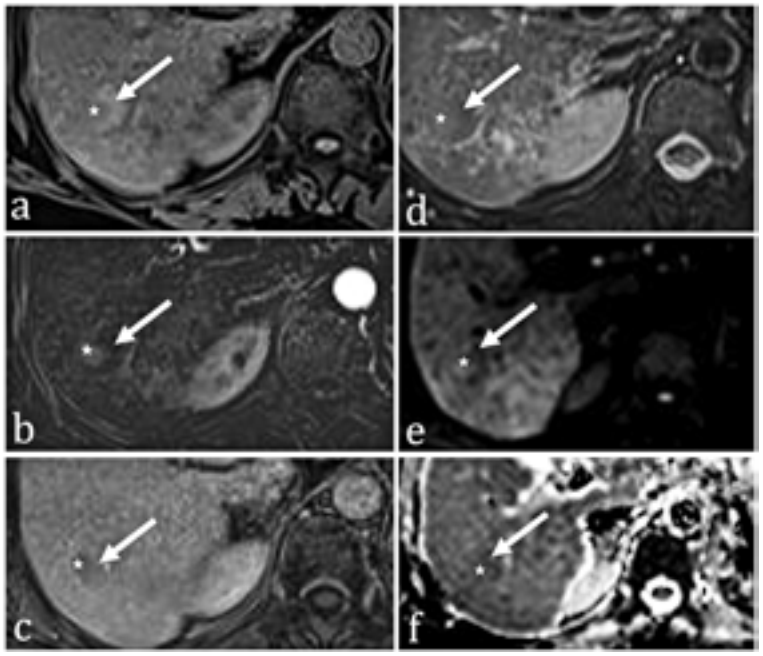

Fig. 2. Imaging features of the nodule after DEB-TACE for a baseline "nodule-in-nodule" HCC: persistent tumoral nidus, but with reduced arterial flash and no restricted diffusion. Arrow – background nodule, * – HCC foci; T1 FatSat images in unenhanced (a), arterial phase - subtraction (b), hepatobiliary phase (c); T2 FatSat images (d); DWI images (e) with ADC map correlation (f).

In our study, we recruited all patients with nodule-in-nodule imaging patterns on their baseline diagnostic scan. These patients were submitted to an MRI examination one month after the TACE procedure. Since no other diagnostic modality such as surgery or biopsy is indicated in these patients, dynamic contrast MRI holds the best sensitivity and specificity in this situation [2, 25]. All patients demonstrated progressive disease at four weeks after the procedure, albeit with various imaging patterns.

The image analysis of the selected patients demonstrated heterogeneous morphological and dynamic contrast patterns. Only 7 out of 9 patients showed T2 WI hyperintensity in the HCC foci, and among them, 6 demonstrated restricted diffusion. The other patient, with no restricted diffusion in the HCC foci, also presented an atypical contrast enhancement pattern, with just moderate and persistent contrast uptake, and without wash-out. In this case (patient 2), the diagnosis of tumor recurrence was made on a size increase of 23% from the baseline, which signified progressive disease according to mRECIST criteria [15]. The absence of diffusion restriction in the HCC foci in our case may be caused by respiration or magnetic susceptibility artifacts [26]. The two patients without T2 WI hyperintensity in the HCC foci demonstrated either a tumor viable tissue size increase (27% in patient 1) or typical arterial flash and portal washout in patient 4, diagnostic criteria for tumor recurrence in both patients.

The signal intensity in T2 WI correlates with the presence of restricted diffusion, and the marginal statistical significance most likely originates from the reduced number of cases and aforementioned artifacts, which may corrupt statistical interpretation. Higher p values in this case predispose the interpreter to a Type I error, since diffusion sequences use a T2 WI mask and new study models demonstrate the interconnectivity between the two sequence types [27].

T1 WI isointensity within the HCC foci was found in two cases, presumably due to liquefaction necrosis material [28] and partial signal summation of HCC foci and the background nodule due to the former's small size (largest diameter of 11 and 12 mm, respectively) and the latter's overall T1 hyperintensity.

The dynamic contrast analysis with hepatocyte-specific media demonstrated a typical pattern (arterial "flash" and portal "wash-out") in 5 cases (Fig. 3). Within the 4 remaining patients, the contrast intensity in the portal phase was similar to the arterial phase in 2 nodules and more intense in the other 2. In these situations, the presence of pseudolesions after TACE with the abnormally inner-nodule signal might have corresponded to granulation tissue. Nevertheless, the follow-up exam showed tumor viable tissue in all cases, albeit the atypical imaging features (Fig. 4). The shape of the contrast-enhanced lesion also holds an important significance when trying to rule out a pseudolesion. Previous studies have demonstrated that a nodular shape is more likely to harbor malignant tissue, when compared with crescent or rim enhancing lesions [29]. We assumed that the placement of the HCC foci inside a larger, predominantly hypovascular nodule, altered the arterial blood flow towards the residual tumor tissue, causing this atypical contrast uptake profile. Also, the average diameter of 14.7 mm of the HCC foci favors atypical imaging features [30].

In our patients we found no correlation between contrast enhancement measured in percentages over the unenhanced phase signal, and the HCC foci size or morphological appearance.

The correct detection of tumor recurrence in the selected patients using only the morphological criteria would be achieved in 7 out of 9 cases, and by using dynamic contrast analysis alone, it would be achieved in just 5 cases. These findings would be alarming when compared to the diagnostic efficiency of MRI for untreated HCC nodules in the cirrhotic liver, or even for TACE treated HCC nodules [31]. But when dealing with nodule-in-nodule baseline architecture with overlapped TACE treatment, more parameters that might influence the imaging aspects should be considered. For instance, the overall

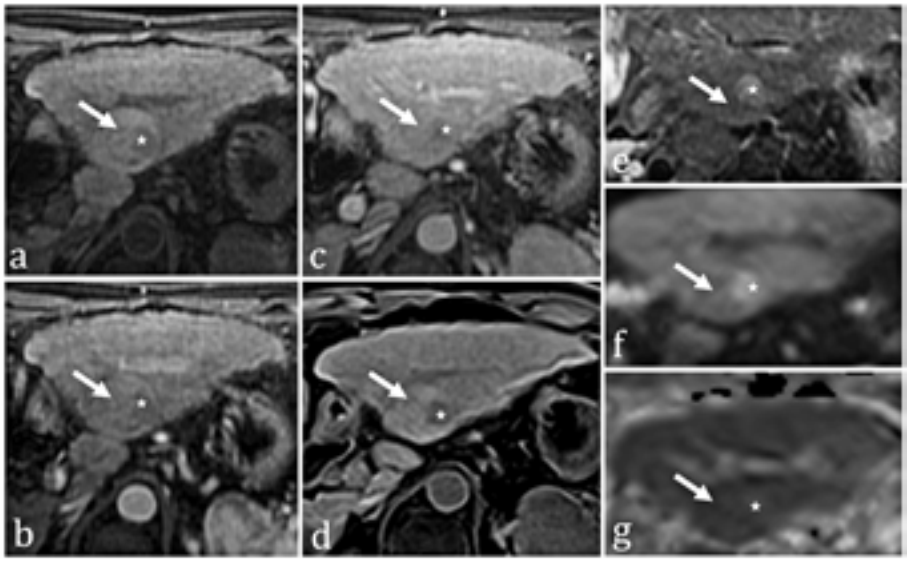

Fig. 3. Nodule-in-nodule imaging pattern after TACE. Certain HCC foci within the larger background nodule, with typical tumoral features: T1 hypointensity/T2 hyperintensity, arterial flash with portal wash-out and late hypointensity, and demonstrating restricted diffusion. Arrow – background nodule, * – HCC foci; T1 FatSat images in unenhanced (a), arterial phase (b), portal venous phase (c), hepatobiliary phase (d); T2 FatSat images (e); DWI images (f) with ADC map correlation (g).

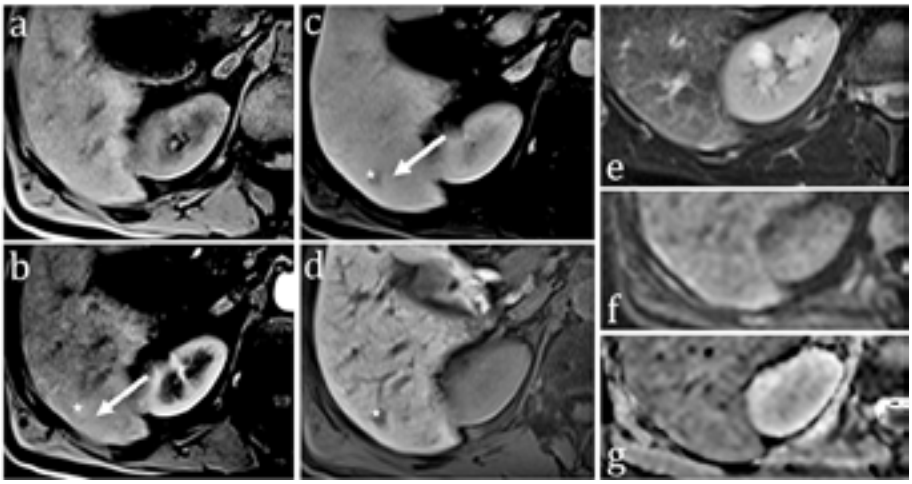

Fig. 4. Less typical imaging features of a nodule-in-nodule pattern demonstrates a background nodule isointense in T2 and T1 WI. The HCC foci show discrete arterial contrast uptake and wash-out in portal venous phase, with hypointensity in the hepatobiliary phase, yet no restricted diffusion. Arrow – background nodule, * – HCC foci; T1 FatSat images in unenhanced (a), arterial phase (b), portal phase (c), late hepatobiliary phase (d); T2 FatSat images (e); DWI images (f) with ADC map correlation (g).

T1 WI hyperintensity of the background nodule, combined with the potential T1 hyperintensity of post interventional necrosis may obscure the arterial flash of the HCC foci, and may also impede the interpretation of tumor wash-out in the portal phase [32]. Another factor is the frequent appearance of pseudolesions, which mimic HCC foci; distinguishing the two is often challenging, and sometimes impossible by imaging alone.

When combining the diagnostic value of morphological and dynamic contrast images, the correct diagnosis of viable tumor tissue was set in 8 out of 9 cases. Adding the size evolution criteria, all patients were diagnosed with tumor viable tissue (100% sensitivity). When using the hepatobiliary phase as a criterion for the presence of HCC, all patients demonstrated marked hypointensity in the inner-nodule at 20 minutes after Acidum Gadoxeticum administration. Literature data demonstrates high sensitivity and specificity for the MRI hepatobiliary phase in detecting malignant hepatic lesions [19, 33]. In our study, the specificity could not be determined due to the lack of a control group.

Alongside morphological and functional MRI markers for the tumor detection, a correct and thorough patient follow-up protocol is essential in the early detection of tumor recurrence. The sequential follow-up imaging protocol may be the only criterion for tumor viable tissue depiction, as demonstrated in this study, when other imaging features may be inconspicuous or confusing. The relative controversy for the best timing and choice of imaging modality in the follow-up protocols should be surpassed by relying on the centers' experience in practice and by a multidisciplinary approach in oncology boards [34, 35].

The study limits are the relatively low number of patients included for this particularly rare sub-type imaging pattern, and the lack of a gold standard test with absolute sensitivity and specificity to validate the MRI findings.

CONCLUSION

The nodule-in-nodule architecture of HCC treated by TACE may demonstrate atypical morphological and functional features of MRI for residual HCC foci. There was an expected correlation between T2 WI hyperintensity and restricted diffusion within the HCC foci.

The diagnostic accuracy for HCC recurrence in TACE-treated patients with nodule-in-nodule baseline imaging patterns was increased when combining T1 WI, T2 WI, DWI and dynamic contrast modalities. The diagnostic yield improved when adding the tumor size increase in follow-up studies, and was maximal when the hepatobiliary phase with Acidum Gadoxeticum was considered.

Conflicts of interest: None to declare. **Funding**: No financial support was received for this study.

Authors' contribution: A.E.S.: study concept and design, data aquisition and interpretation; A.E.S. and C.S.: manuscript writing; C.S.: statistical analysis; I.G.L.: study supervision and coordination, critical revision of the manuscript for important intellectual content before submission. All authors approved the final version of the manuscript.

REFERENCES

1. Jemal A, Bray F, Center MM, et al. Global cancer statistics. CA Cancer J Clin 2011;61:69-90. doi:10.3322/caac.20107
2. Poon D, Anderson BO, Chen LT, et al. Management of hepatocellular carcinoma in Asia: consensus statement from the Asian Oncology Summit 2009. Lancet Oncol 2009;10:1111-1118. doi:10.1016/S1470-2045(09)70241-4
3. Takayasu K, Arii S, Ikai I, et al. Prospective cohort study of transarterial chemoembolization for unresectable hepatocellular carcinoma in 8510 patients. Gastroenterology 2006;131:461-469. doi:10.1053/j.gastro.2006.05.021
4. Pons F, Varela M, Llovet JM. Staging systems in hepatocellular carcinoma. HPB (Oxford) 2005;7:35-41. doi:10.1080/13651820410024058
5. Pelletier G, Ducreux M, Gay F, et al. Treatment of unresectable hepatocellular carcinoma with lipiodol chemoembolization: a

multicenter randomized trial. Groupe CHC. J Hepatol 1998;29:129-134. doi:10.1016/S0168-8278(98)80187-6
6. Halpenny DF, Torreggiani WC. The infectious complications of interventional radiology based procedures in gastroenterology and hepatology. J Gastrointestin Liver Dis 2011;20:71-75.
7. Kline TL, Knudsen BE, Anderson JL, Vercnocke AJ, Jorgensen SM, Ritman EL. Anatomy of hepatic arteriolo-portal venular shunts evaluated by 3D micro-CT imaging. J Anat 2014;224:724-731. doi:10.1111/joa.12178
8. Lo CM, Ngan H, Tso WK, et al. Randomized controlled trial of transarterial lipiodol chemoembolization for unresectable hepatocellular carcinoma. Hepatology 2002;35:1164-1171. doi:10.1053/jhep.2002.33156
9. Efremidis SC, Hytiroglou P. The multistep process of hepatocarcinogenesis in cirrhosis with imaging correlation. Eur Radiol 2002;12:753-764. doi:10.1007/s00330-001-1142-z
10. Campos JT, Sirlin CB, Choi JY.Focal hepatic lesions in Gd-EOB-DTPA enhanced MRI: the atlas. Insights Imaging 2012;3:451-474. doi:10.1007/s13244-012-0179-7
11. Hernández-Guerra M, Hernández-Camba A, Turnes J, et al. Application of the Barcelona Clinic Liver Cancer therapeutic strategy and impact on survival. United European Gastroenterol J 2015;3:284-293. doi:10.1177/2050640615575971
12. Albiin N. MRI of Focal Liver Lesions. Curr Med Imaging Rev 2012;8:107-116. doi:10.2174/157340512800672216
13. Saito K, Tajima Y, Harada TL. Diffusion-weighted imaging of the liver: Current applications. World J Radiol 2016;8:857-867.
14. Shapiro SS, Wilk MB. An Analysis of Variance Test for Normality (Complete Samples). Biometrika 1965;52:591-611. doi:10.2307/2333709
15. Sato Y, Watanabe H, Sone M, et al. Tumor response evaluation criteria for HCC (hepatocellular carcinoma) treated using TACE (transcatheter arterial chemoembolization): RECIST (response evaluation criteria in solid tumors) version 1.1 and mRECIST (modified RECIST): JIVROSG-0602. Ups J Med Sci 2013;118:16-22. doi:10.3109/03009734.2012.729104
16. Koh DM, Collins DJ. Diffusion-weighted MRI in the body: applications and challenges in oncology. AJR Am J Roentgenol 2007;188:1622-1635. doi:10.2214/AJR.06.1403
17. Willatt JM, Hussain HK, Adusumilli S, Marrero JA. MR Imaging of hepatocellular carcinoma in the cirrhotic liver: challenges and controversies. Radiology 2008;247:311-330. doi:10.1148/radiol.2472061331
18. Yoon JH, Lee JM, Yu MH, Kim EJ, Han JK. Triple Arterial Phase MR Imaging with Gadoxetic Acid Using a Combination of Contrast Enhanced Time Robust Angiography, Keyhole, and Viewsharing Techniques and Two-Dimensional Parallel Imaging in Comparison with Conventional Single Arterial Phase. Korean J Radiol 2016;17:522-532. doi:10.3348/kjr.2016.17.4.522
19. Giuga M, De Gaetano AM, Guerra A, et al. An update on clinical applications of hepatospecific contrast media in magnetic resonance imaging of liver parenchyma. Eur Rev Med Pharmacol Sci 2016;20:2515-2525.
20. Choi JY, Lee JM, Sirlin CB. CT and MR imaging diagnosis and staging of hepatocellular carcinoma: part II. Extracellular agents, hepatobiliary agents, and ancillary imaging features. Radiology 2014;273:30-50. doi:10.1148/radiol.14132362
21. Scheau AE, Scheau C, Dumitru RL, Dima SO, Lupescu IL. Tumor response criteria for hepatocellular carcinoma treated by transarterial chemoembolization - a radiologist's point-of-view. J Transl Med Res 2015;20:8-18. doi:10.21614/jtmr-20-1-24
22. Efremidis SC, Hytiroglou P, Matsui O. Enhancement patterns and signal-intensity characteristics of small hepatocellular carcinoma in cirrhosis: pathologic basis and diagnostic challenges. European Radiology 2007;17:2969-2982. doi:10.1007/s00330-007-0705-z
23. Terada T, Kadoya M, Nakanuma Y, Matsui O. Iron-accumulating adenomatous hyperplastic nodule with malignant foci in the cirrhotic liver. Histopathologic, quantitative iron, and magnetic resonance imaging in vitro studies. Cancer 1990;65:1994-2000. doi:10.1002/1097-0142(19900501)65:9<1994::AID-CNCR2820650919>3.0.CO;2-B
24. Sano K, Ichikawa T, Motosugi U, et al. Imaging Study of Early Hepatocellular Carcinoma: Usefulness of Gadoxetic Acid–enhanced MR Imaging. Radiology 2011;261:834-844. doi:10.1148/radiol.11101840
25. Lee YJ, Lee JM, Lee JS, et al. Hepatocellular carcinoma: diagnostic performance of multidetector CT and MR imaging-a systematic review and meta-analysis. Radiology 2015;275:97-109. doi:10.1148/radiol.14140690
26. Kamel IR, Bluemke DA, Ramsey D, et al. Role of diffusion-weighted imaging in estimating tumor necrosis after chemoembolization of hepatocellular carcinoma. AJR Am J Roentgenol 2003;181:708-710. doi:10.2214/ajr.181.3.1810708
27. Cheng L, Blackledge MD, Collins DJ, et al. T2-adjusted computed diffusion-weighted imaging: A novel method to enhance tumour visualisation. Comput Biol Med 2016;79:92-98. doi:10.1016/j.compbiomed.2016.09.022
28. Lee JM, Trevisani F, Vilgrain V, Wald C. Imaging diagnosis and staging of hepatocellular carcinoma. Liver Transpl 2011;17 Suppl 2:S34-S43. doi:10.1002/lt.22369
29. Bonekamp D, Bonekamp S, Halappa VG, et al. Interobserver agreement of semi-automated and manual measurements of functional MRI metrics of treatment response in hepatocellular carcinoma. Eur J Radiol 2014;83:487-496. doi:10.1016/j.ejrad.2013.11.016
30. Choi MH, Choi JI, Lee YJ, Park MY, Rha SE, Lall C. MRI of Small Hepatocellular Carcinoma: Typical Features Are Less Frequent Below a Size Cutoff of 1.5 cm. AJR Am J Roentgenol 2017;208:544-551. doi:10.2214/AJR.16.16414
31. Bargellini I, Battaglia V, Bozzi E, Lauretti DL, Lorenzoni G, Bartolozzi C. Radiological diagnosis of hepatocellular carcinoma. J Hepatocell Carcinoma 2014;1:137-148. doi:10.2147/JHC.S44379
32. Quaia E, De Paoli L, Pizzolato R, et al. Predictors of dysplastic nodule diagnosis in patients with liver cirrhosis on unenhanced and gadobenate dimeglumine–enhanced MRI with dynamic and hepatobiliary phase. AJR Am J Roentgenol 2013;200:553-562. doi:10.2214/AJR.12.8818
33. An C, Rhee H, Han K, et al. Added value of smooth hypointense rim in the hepatobiliary phase of gadoxetic acid-enhanced MRI in identifying tumour capsule and diagnosing hepatocellular carcinoma. Eur Radiol 2017;27:2610-2618. doi:10.1007/s00330-016-4634-6
34. El-Serag HB, Davila JA. Surveillance for hepatocellular carcinoma: in whom and how? Therap Adv Gastroenterol 2011;4:5-10. doi:10.1177/1756283X10385964
35. Kalb B, Chamsuddin A, Nazzal L, Sharma P, Martin DR. Chemoembolization follow-up of hepatocellular carcinoma with MR imaging: usefulness of evaluating enhancement features on one-month posttherapy MR imaging for predicting residual disease. J Vasc Interv Radiol 2010;21:1396-1404. doi:10.1016/j.jvir.2010.05.015